A Local ROI-specific Atlas-based Segmentation of Prostate Gland and Transitional Zone in Diffusion MRI

Junjie Zhang[1], Sameer Baig[1], Alexander Wong[2], Masoom A. Haider[1], Farzad Khalvati[1]

[1]Dept. of Medical Imaging, Sunnybrook Research Institute, University of Toronto, Toronto, ON, Canada

[2]Dept. of System Design Engineering, University of Waterloo, Waterloo, ON, Canada

Abstract

Segmentation of prostate and related anatomic structure, such as transitional zone, in medical images facilitates prostate cancer detection, as well as a number of other clinical practices. In this paper, we propose a semi-automatic local ROI-specific atlas-based segmentation (LABS) method to segment prostate gland and transitional zone in diffusion magnetic resonance images. Inspired by a sequential registration-based segmentation method, the proposed method further reduces the amount of user intervention and focuses on the vicinity of prostate for atlas matching and atlas-to-target registration by specifying the bounding boxes of prostate gland on key slices of volume images. We evaluated the method on an atlas database with the 100 cases by performing a leave-one-out study. Our proposed method produced favorable outcomes with an average Dice similarity coefficient of 0.85±0.03 for prostate gland and 0.77±0.06 for transitional zone segmentations, which indicates the effectiveness of the proposed method and its potential to be used in relevant clinical applications.

1. Introduction

Accurate localization and segmentation of the prostate gland and related anatomic structures, such as transitional zone, in medical images is needed in different phases of clinical practices for prostate cancer diagnosis, treatment, and monitoring [1]. In computer-aided prostate cancer detection, it is usually the first step to segment prostate from the medical images [2]. In treatment planning for radiation therapy, delineation of prostate is usually performed on magnetic resonance (MR) images, for their superior soft-tissue contrast to computed tomography (CT) images [3].

The current practice of manually contouring the prostate gland in MR images is a tedious task. The long time required to process and delineate the volumetric datasets of prostate images by clinicians imposes a serious burden on the healthcare system and prevents timely patient access to proper care. The availability of a computer-assisted segmentation method could reduce the time spent manually contouring the prostate gland and potentially reduce the inter-user variability of diagnosis [4].

A popular class of algorithms in literature for prostate segmentation is *atlas-based segmentation* (ABS) algorithms [5]. Briefly, this method first constructs a database, or an "atlas", containing the original images with corresponding labels (i.e., segmented binary images) of desired anatomy (e.g., prostate) contoured by experts. To segment the prostate in a target image, all of the images in the atlas are registered to the target image using an image registration method. The registered images in the atlas are then compared to the target image using an image similarity matching technique to find the most similar registered image in the atlas. Once the matched registered image is selected, the corresponding image transformation is applied to the original segmented images (or labels) to produce the registered labels as the final segmentation.

ABS makes use of a large set of contours from experts as prior knowledge, and generally assumes that registration will eliminate the differences between images (i.e., atlas images and the target image). However, the registration between atlas images and the target image, in particular for MR images, can be difficult, if not a failure, due to several factors. Those factors include large variability of the MR images in terms of image intensity characteristics (e.g. scanner variability), structure (e.g., different field of views (FOVs) and different imaging center), and anatomical variabilities of scanned regions.

To overcome these limitations and to make image registration more robust, we propose a semi-automatic *local ROI-specific atlas-based segmentation* (LABS) method to segment prostate gland and transitional zone in diffusion MR images. This method is inspired by ABS and a *sequential registration-based segmentation* (SRS) method proposed in [4,6]. Instead of pre-generating an atlas, SRS makes initial contours on some key slices of a patient's volume images. Then it propagates a given label (or segmentation) to its neighboring slices exploiting the inter-slice similarity. Rather than contouring the exact segments similar to SRS, our method proposes to further reduce the amount of user intervention, by only specifying the bounding boxes of prostate gland on key slices (e.g., the base, middle, and the apex). A user specified ROI volume is then generated by propagating the ROIs through the slices. Thus, in addition to minimizing user intervention, we focus only on the vicinity of prostate for atlas matching and atlas-to-target registration to ensure better correlation of ROIs and increase the accuracy in registration and hence, segmentation.

In the following, we will describe details of our pipeline in Section 2, and present the experimental results in Section 3. Section 4 discusses and concludes the paper.

2. Methods

We describe the proposed method in this section. The whole pipeline is depicted in Fig. 1. In this figure, the gray box contains the pre-segmented atlas database. The four main steps of the pipeline are contained in the four colored boxes.

Step I: User-specified Bounding Box

In the first step, the user specifies the bounding boxes (BBs) of the prostate gland on some key slices. It is important to correctly locate the first and last slices in which the base and the apex of the prostate appear. Identifying the slice in mid-gland region with largest cross sections is also essential. At least 3 BBs in the beginning, middle and end of the gland are needed to produce the prostate volume of interest (VOI) by interpolating the BBs across slices. Specifying extra BBs on more slices will increase the accuracy of segmentation. In practice, the ROI on each slice is enlarged (i.e., by 100%) to ensure the whole prostate region is covered on the corresponding slice in atlas images.
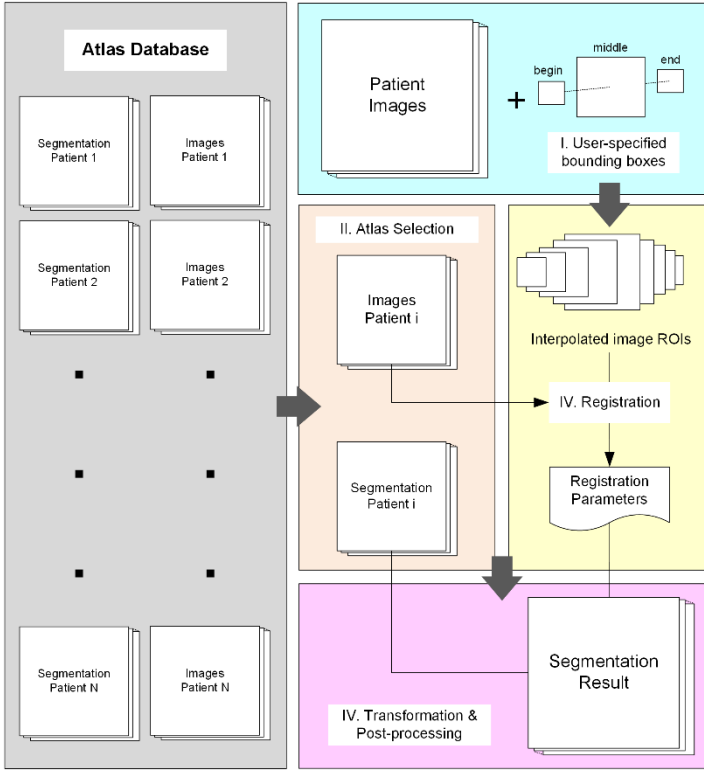
Fig. 1: The proposed pipeline. We specify the region-of-interests (ROIs) of patient images by interpolating the user-drawn bounding boxes of prostate gland (I). All the consequent image matching (II), registration (III), and transformation (IV) is focused on the local specific image ROIs.

Step II: Atlas Selection

The corresponding prostate VOIs for each patient images in the atlas database is first extracted with respect to the prostate VOI of target images. Then a selection is made of VOI images in the atlas that are most similar to the VOI images of the target patient. The selection is made based on two criteria: the similarity measurement (i.e., correlation coefficients, Eq. (1)) and volume ratio (see Eq. (2)) between the prostate VOIs of the atlas and that of the target images:

$$Corr(I_A, I) = \frac{\sum_{i=1}^{m}\sum_{j=1}^{n}(I_A - \overline{I_A})(I - \bar{I})}{\sqrt{\left(\sum_{i=1}^{m}\sum_{j=1}^{n}(I_A - \overline{I_A})^2\right)\left(\sum_{i=1}^{m}\sum_{j=1}^{n}(I - \bar{I})^2\right)}} \quad (1)$$

where m and n are the row and column of images I_A and I, $\overline{I_A}$ and $\bar{I}$ are the mean values of images I_A and I. The similarity measure is the average correlation coefficients of all ROIs between the selected atlas and target images.

Volume ration is defined as:

$$V_{ratio}(\%) = \frac{V_A}{V} \times 100 \quad (2)$$

where V_A is the volume of the prostate VOI of atlas images and V is that of the target images. The corresponding atlas whose prostate VOI has the highest correlation with the target images VOI while its volume ratio is within a certain range (i.e., $100\pm25\%$) is selected as the best matched atlas.

Step III. ROI-based Registration

In this stage, the registration is carried similar to typical ABS method, but it is constrained to the enlarged user-specified ROIs. Each image I_A^i in the constructed VOI of the selected atlas images

is registered to that I^i of the VOI of the target images, using a registration method as follows:

$$T_i = Reg(I_A^i, I^i) \quad (3)$$

where Reg is an affine registration method and $i \in \{1, 2, ..., n\}$ and n is the number slices in the target images. The computed registration transformation, T_i, is then applied to labels of atlas VOI to produce the registered/deformed label VOI in Step IV.

Step IV: Transformation and Post-processing

Before we put the transformed label VOI (or mask) back onto each target image to form the final segmentation result, we add a post-processing step to scale the label mask (with label=1 representing the prostate) back to the size of interpolated bounding box. It is supposed the post-processing step could further increase the localization accuracy of the label mask, and hence, the segmentation result. The segmentation results of prostate gland and transitional zone with and without the post-processing are presented in Section 3.

3. Experimental Results

The entire LABS pipeline was implemented and integrated into ProCanVAS (Prostate Cancer Visualization and Analysis System) platform, developed at Sunnybrook Research Institute, Toronto, ON, Canada. The platform is a complete clinical decision support system, providing a set of tools for computational diffusion MRI, image contouring (manually and semi-automatically, i.e. LABS), image feature extraction, and prostate cancer detection (Fig. 2).
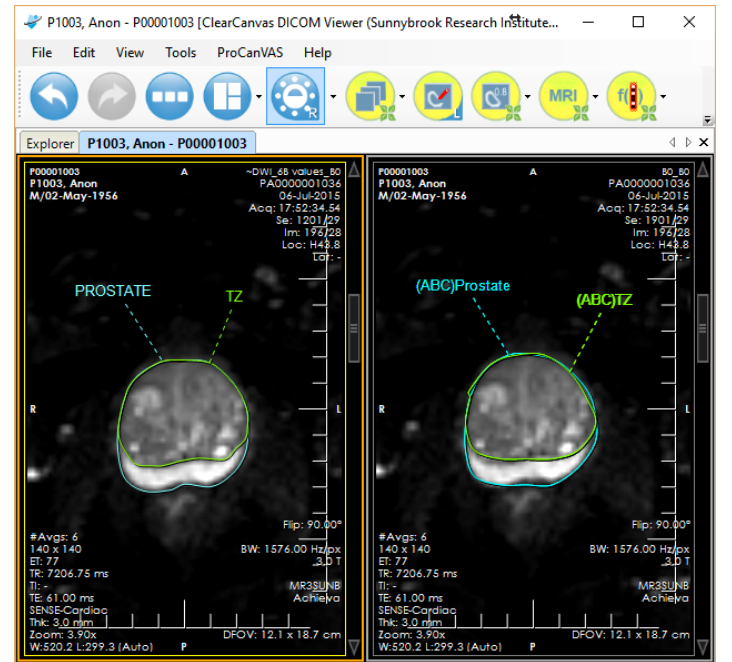

Fig. 2: The prostate gland and transitional zone (TZ) generated by LABS in ProCanVAS (Right). Left image shows the manual segmentation (ground truth).

The proposed LABS method was evaluated on 100 patients' diffusion-weighted MRI data via a leave-one-out cross validation. The images were acquired using a Philips Achieva 3.0T machine at Sunnybrook Health Sciences Centre, Toronto, ON, Canada. All data was obtained under the local institutional research ethics board.

The prostate glands and transitional zones of images of 100 patients' diffusion-weighted MRI data ($b = 0s/mm^2$) were manually contoured by an expert using ProCanVAS platform. A leave-one-out cross validation was implemented to generate labels for prostate gland and transitional zone for each case using the remaining 99 patients' images as the atlas database. Fig. 2 shows an example of the segmentation result of the prostate gland and transitional zone in ProCanVAS (right), with manual contoured (ground truth) displayed on the left side.

The performance of LABS was evaluated by comparing the semi-automatically generated segmentations for both the prostate gland and transitional zone with the ground-truth labels using Dice similarity coefficient (DSC), the well-known measure of segmentation overlap defined as:

$$DSC(S_L, S_G) = \frac{2|S_L \cap S_G|}{|S_L| + |S_G|} \qquad (4)$$

where S_L and S_G represent the segmentation generated by the proposed LABS method and the ground-truth, respectively. $\cap$ denotes the shared information in the two binary images. DSC ranges from 0 (no overlap) to 1 (perfect overlap). A higher DSC indicates a better correspondence.

In our experiment, we produced results with both 3 and 5 user-specified bounding boxes, and the segmentation results with (w.) and without (w/o. or original) post-processing. The accuracy results are presented in Tables 1 and 2 and Fig. 3.

Table 1. DSC (%) of prostate gland segmentation.

	3 BBs	5 BBs	$\overline{\Delta DSC}$
w/o. post-processing	**76.8**±8.2	**78.3**±6.5	+1.5
w. post-processing	**80.2**±4.7	**85.4**±3.2	+5.2
$\overline{\Delta DSC}$	+3.4	+7.1	

Table 2. DSC (%) of transitional zone segmentation.

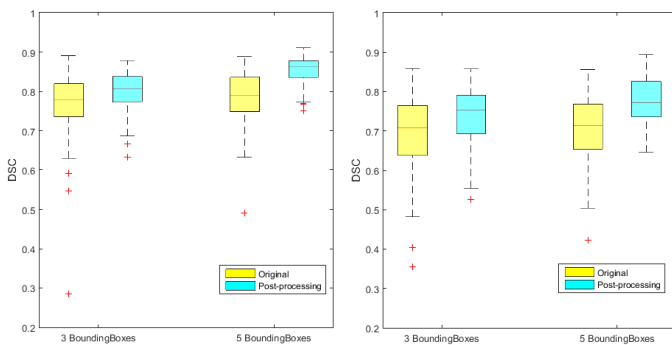|	3 BBs	5 BBs	$\overline{\Delta DSC}$
w/o. post-processing	**69.1**±9.6	**70.6**±8.4	+1.5
w. post-processing	**73.7**±6.8	**77.3**±5.9	+3.6
$\overline{\Delta DSC}$	+4.6	+6.8	

Fig. 3: Results (DSC) for prostate gland (left) and transitional zone (right) segmentation. Each boxplot shows the effect of number of user-specified bounding boxes and with/without post-processing on the segmentation results.

Tables 1 and 2 show the average value of DSC with standard deviation of the LABS generated segmentations of prostate gland and transitional zone, compared with ground truth, respectively, under different experimental configurations. Final segmentations with 5 user-specified BBs and post-processing exhibit the highest average DSCs with smallest standard deviations for both cases (prostate: 85.4±3.2, and transitional zone: 77.3±5.9). Fig. 3 shows

the trend clearly: segmentations with 5 user-specified BBs always outperform those with 3 user-specific BBs, and post-processing could further boost the segmentation accuracy in the final stage. The improvement by post-processing is more significant for 5 user-specified BBs cases, which could be due to the fact that more user-specified BBs enable a more accurate localization of the prostate gland during the interpolation of ROIs. Compared with prostate gland, the segmentation results of transitional zone have lower average DSCs and higher standard deviations. This is not surprising due to the relative ambiguous boundaries of transitional zones in anatomical structure in the prostate gland, which contribute to the difficulty in segmenting them accurately.

4. Conclusions

In this paper, we proposed a semi-automatic local ROI-specific atlas-based (LABS) algorithm for prostate gland and transitional zone segmentation in diffusion MR images. Inspired by a sequential registration-based segmentation method, our proposed method attempts to further reduce the amount of user intervention and increase the registration accuracy by focusing on the vicinity of prostate region for atlas matching and atlas-to-target registration using user-specified bounding boxes on key slices. The proposed LABS method was evaluated on an atlas database with 100 cases by performing a leave-one-out cross validation. Compared with the manual ground-truth segmentation, our proposed method produced favorable outcomes with an average Dice similarity coefficient 0.85±0.03 for prostate gland segmentation and 0.77±0.06 for transitional zone segmentation. The results show that the proposed algorithm could be used to aid the prostate gland and transitional zone segmentation in diffusion MR images, with great potential to improve the efficiency and reduce the inter-user variability of prostate cancer diagnosis.

References

[1] Langer, D. L., van der Kwast, T. H., Evans, A. J., Trachtenberg, J., Wilson, B. C., & Haider, M. A. (2009). Prostate cancer detection with multi-parametric MRI: logistic regression analysis of quantitative T2, diffusion-weighted imaging, and dynamic contrast-enhanced MRI. Journal of Magnetic Resonance Imaging: JMRI, 30(2), 327–34.

[2] Zhang, J., Khalvati, F., Wong, A., & Haider, M. A. (2015). Superpixel-based Prostate Cancer Detection from Diffusion Magnetic Resonance Imaging. Vision Letters, 1(1), VL107.

[3] Hentschel, B., Oehler, W., Strauf, D., Ulrich, A., & Malich, A. (2011). Definition of the CTV prostate in CT and MRI by using CT-MRI image fusion in IMRT planning for prostate cancer. Strahlentherapie Und Onkologie, 187(3), 183–190.

[4] Khalvati, F., Salmanpour, A., Rahnamayan, S., Haider, M. A., & Tizhoosh, H. R. (2016). Sequential Registration-Based Segmentation of the Prostate Gland in MR Image Volumes. Journal of Digital Imaging, 29(2), 254–263.

[5] Klein, S., van der Heide, U. a, Lips, I. M., van Vulpen, M., Staring, M., & Pluim, J. P. W. (2008). Automatic segmentation of the prostate in 3D MR images by atlas matching using localized mutual information. Medical Physics, 35(4), 1407–1417.

[6] Khalvati, F., Salmanpour, A., Rahnamayan, S., Rodrigues, G., & Tizhoosh, H. R. (2013). Inter-slice bidirectional registration-based segmentation of the prostate gland in MR and CT image sequences. Medical Physics, 40(12), 123503.